

A Hemimethyl-Substituted Cucurbit[7]uril Derived from 3 α -Methylglycoluril

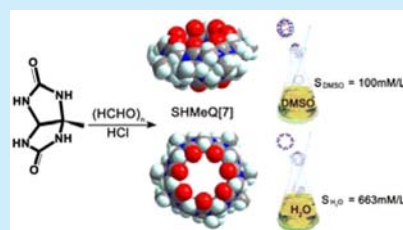
Wen-Xuan Zhao,[†] Chuan-Zeng Wang,[†] Li-Xia Chen,[†] Hang Cong,[†] Xin Xiao,[†] Yun-Qian Zhang,[†] Sai-Feng Xue,[†] Ying Huang,[‡] Zhu Tao,^{*,†} and Qian-Jiang Zhu^{*,†}

[†]Key Laboratory of Macrocyclic and Supramolecular Chemistry of Guizhou Province, Guizhou University, Guiyang 550025, China

[‡]The Engineering and Research Center for Southwest Bio-Pharmaceutical Resources of National Education Ministry of China, Guizhou University, Guiyang 550025, China

S Supporting Information

ABSTRACT: A novel hemimethyl-substituted cucurbit[7]uril (HMeQ[7]) derived from 3 α -methylglycoluril has been prepared. HMeQ[7] is readily soluble in both water and dimethyl sulfoxide (DMSO) and displays not only host–guest interaction properties similar to those of the normal cucurbit[7]uril but also unusual properties in DMSO.



Cucurbit[7]uril (Q[7]) has been extensively investigated in host–guest interaction chemistry^{1–5} and coordination chemistry^{6,7} due to its modest water solubility (20–30 mM) and relatively large cavity. Indeed, of all of the reports, articles, patents, etc. relating to cucurbit[*n*]uril chemistry, since its discovery in 2000, over 30% have dealt with Q[7].^{8,9} Currently, research concerning Q[7] is directed toward various areas in which, for example, it is used to effectively encapsulate and stabilize a wide range of molecules, such as fluorescent dyes,¹⁰ making it applicable to light-harvesting systems;¹¹ it can also serve as a drug delivery vehicle¹² and enhances the bioavailability of drugs.^{5,13} Although Q[7] can be dissolved in neutral water, it is insoluble in organic solvents. In 2003, Kim and co-workers reported perhydroxylated cucurbit[7]uril, (HO)₁₄Q[7], which was obtained by the direct oxidation of Q[7] with K₂S₂O₈ in water and proved to be soluble in water as well as in other solvents, such as DMSO.¹⁴ However, the poor yield frustrated extensive research on this novel Q[7] derivative.^{15,16} In recent years, Isaacs and co-workers have established a building-block approach and have synthesized a series of functionalized Q[7] derivatives by the condensation of a methylene-bridged glycoluril hexamer and diethers of substituted glycoluril;^{17–19} the thus obtained Me₂Q[7] displayed extraordinary solubility in water (264 mM).

3 α -Methylglycoluril is a relatively inexpensive glycoluril, and partially methyl-substituted Q[*n*]s derived therefrom (hemimethyl-substituted Q[*n*]s) may be formed in numerous isomers, which may be difficult to separate since they differ only in the orientation of a single methyl substituent on the back of 3 α -methylglycoluril (see Figure S1, Supporting Information, isomers: 4 for HemiMeQ[5]s, 9 for HemiMeQ[6]s, and 10 for HemiMeQ[7]s). However, our previous²⁰ and recent²¹ works revealed that only limited numbers of isomers of hemimethyl-substituted Q[*n*]s could be

formed. For example, only two isomers of HemiMeQ[5]s and two isomers of HemiMeQ[6]s have been found so far. Although we observed HemiMeQ[7]s in our early work,²⁰ the inherent challenge in the separation of the hemimethyl-substituted Q[*n*]s delayed research on these derivatives. In the present work, we have devised an effective approach for the separation of mixtures of hemimethyl-substituted Q[*n*]s that involves sequential elution through columns of Dowex (H⁺) and then silica gel (see the details in the experimental section, Supporting Information). Unexpectedly, a mixture of HemiMeQ[5]s, HemiMeQ[6]s, and HemiMeQ[7]s could be separated into two groups on a Dowex (H⁺) column; the first group consisted of HemiMeQ[6]s,²¹ and the second group consisted of HemiMeQ[5]s and HemiMeQ[7]s, which could be readily separated on a column of silica gel (Figure S2, Supporting Information). Recently, we successfully isolated the inverted Q[6] from the normal Q[6]²² and the inverted Q[7] from a water-soluble mixture of Q[*n*]s, including Q[5], Q[7], tQ[14], etc.²³ Such effective separation could be attributed to the subtle differences in the outer surface electrostatic distributions of the Q[*n*]s, where one of the methine groups from their electrostatically positive glycoluril moieties protrude into the cavities of the inverted Q[*n*]s. Similarly, different orientations of methyl groups on the back of HemiMeQ[*n*]s or the differences of the electrostatics/pK_a at the portals could lead to differences in their outer surface electrostatic distributions resulting in reversals of the eluting orders.

HMeQ[7] can adopt ten geometric isomers (Figure S1, Supporting Information), and the orientations of the methyl groups on the back of an HMeQ[7] isomer can be effectively recognized by crystal structure determination. In recent years,

Received: September 8, 2015

Published: October 8, 2015

our group has developed a polychloride transition metal anion-induced strategy to prepare single crystals of coordination complexes of $Q[n]$ s with various metal ions and their supramolecular assemblies.²⁴ In the present work, we selected $CdCl_2$ as the transition metal source, which can form the $[CdCl_4]^{2-}$ anion in concentrated HCl solutions (>3 M). However, no crystals of HMeQ[7] were formed in such media, due to its higher solubility therein. Fortunately, we could obtain the crystal structure of compound **1** containing the isolated HMeQ[7] in 2 M HCl solution, in which $[Cd_2Cl_8]^{4-}$ anions were formed. Although the so-called “honeycomb effect” of the anions was not observed in the HMeQ[7]-based supramolecular assembly,^{6,24} the $[Cd_2Cl_8]^{4-}$ anions were seen to surround the HMeQ[7] molecules, resulting in the formation of a supramolecular chain of HMeQ[7] molecules with $[Lu(H_2O)_7]^{3+}$ complexes (Figure 1). Figure 1a and b show

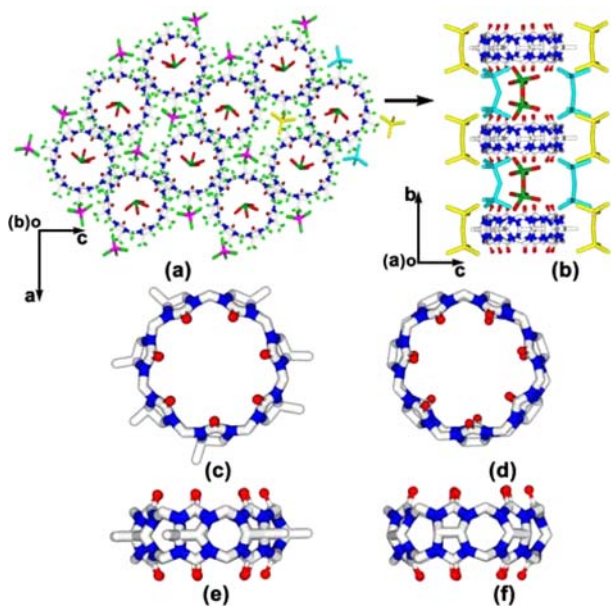


Figure 1. Crystal structures of (a) the overall supramolecular assembly of the HMeQ[7]- $[Cd_2Cl_8]^{4-}$ - $[Lu(H_2O)_7]^{3+}$ system and (b) the HMeQ[7]- $[Lu(H_2O)_7]^{3+}$ supramolecular chain surrounded by four $[Cd_2Cl_8]^{4-}$ chains; (c, e) HMeQ[7] and (d, f) Q[7].

the overall supramolecular assembly constructed of HMeQ[7] molecules, $[Cd_2Cl_8]^{4-}$ anions, and $[Lu(H_2O)_7]^{3+}$ complexes. One can see that each HMeQ[7]- $[Lu(H_2O)_7]^{3+}$ chain is surrounded by four $[Cd_2Cl_8]^{4-}$ chains. In turn, every six HMeQ[7]- $[Lu(H_2O)_7]^{3+}$ chains surround two $[Cd_2Cl_8]^{4-}$ chains. The driving force is attributed to the electropositive outer surface of the HMeQ[7] molecules and $[Lu(H_2O)_7]^{3+}$ cations.²⁴ Energy-dispersive spectrometry (EDS) confirmed that the crystals contained both cadmium (4.93%) and lutetium (4.21%), consistent with the result of the crystal structure determination (Figure S3 and Table S1, Supporting Information). Figure 1c and e show the crystal structure of the isolated HMeQ[7] molecule. Compared to the unsubstituted Q[7] (Figure 1d and f), HMeQ[7] is characterized by seven protruding methyl groups, which impart it with an asymmetric conformation that could enhance its solubility in water. Indeed, experimental results confirmed that the obtained HMeQ[7] displays high solubility in water, in excess of 663 mM at room temperature. Moreover, HMeQ[7] also shows good solubility in DMSO (ca. 100 mM). These outstanding solubilities suggest

that HMeQ[7] could be used in various applications in biochemistry. The powder X-ray diffraction (PXRD) patterns of representative crystals of **1**, and comparison with a simulation, showed that the sample essentially consisted of a pure crystalline phase (Figure S4, Supporting Information). Thermal analysis was used to generate DSC and TG curves of representative crystals. There were no significant differences between those of HMeQ[7] and Q[7] (Figure S5, Supporting Information). Furthermore, FT-IR spectra showed that the highest-wavenumber absorption band of the portal carbonyl groups was different for the two Q[7]s (Figure S6, Supporting Information).

Figure 2 shows the 1H and ^{13}C NMR spectra of HMeQ[7] in D_2O and $DMSO-d_6$, respectively. The 1H NMR spectrum of

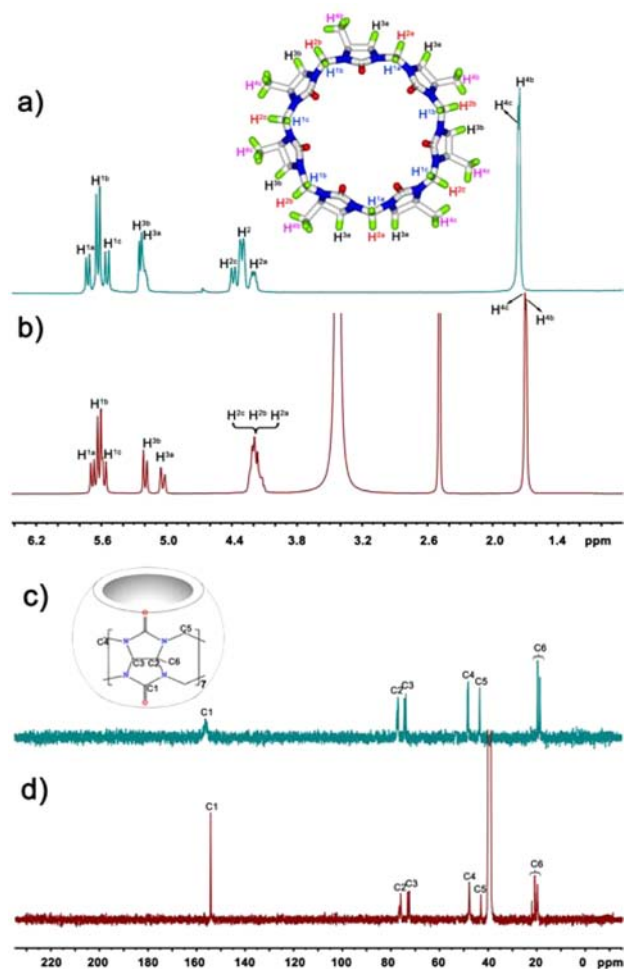


Figure 2. (a, b) 1H NMR spectra of HMeQ[7] in D_2O and $DMSO-d_6$; (c, d) ^{13}C NMR spectra of HMeQ[7] in D_2O and $DMSO-d_6$.

HMeQ[7] in D_2O (Figure 2a) shows four groups of proton resonances in an intensity ratio of about 2:2:1:3, two methylene group signals in the ranges $\delta = 5.55$ – 5.75 and 4.16 – 4.37 ppm, methine group signals in the range $\delta = 5.14$ – 5.22 ppm, and a doublet at $\delta = 1.73$ – 1.75 ppm due to the methyl groups on the back of HMeQ[7]. In $DMSO$, however, the methine proton resonances are split into two doublets in the range $\delta = 5.02$ – 5.21 ppm, and the methylene group signal at high field is broadened (Figure 2b). Detailed assignments can be observed from the ROESY spectrum as shown in Figure S7, Supporting Information. The ^{13}C NMR spectra of HMeQ[7] in both D_2O

and DMSO- d_6 (Figure 2c and d) also feature four groups of resonances: the carbonyl carbon resonances (C1) in the range $\delta = 154.24$ – 156.24 ppm, the methine groups signals (C2, C3) in the range $\delta = 72.39$ – 77.20 ppm, the methylene group signals (C4, C5) in the range $\delta = 42.90$ – 53.22 ppm, and the methyl group signals (C6) in the range $\delta = 18.72$ – 22.05 ppm. Matrix-assisted laser desorption ionization time-of-flight mass spectrometry (MALDI-TOF) of the new species HMeQ[7] gave ions that were equivalent to an HMeQ[7] molecule (for the HMeQ[7]– K^+ ion, $m/z = 1300$ and for the HMeQ[7]– CH_3COOH – K^+ inclusion ion, $m/z = 1360$, as shown in Figure S8, Supporting Information).

The geometric parameters of HMeQ[7], such as portal width, cavity capacity, and height, were found to be similar to those of normal Q[7] (Table S2, Supporting Information). Therefore, HMeQ[7] can be expected to display similar host–guest interaction properties to those of normal Q[7]. Three typical representative guests, namely the chloride salts of 1,6-diaminohexane (g1), 4,4'-bipyridine (g2), and adamantamine (g3), were selected for investigation of the host–guest interaction in water and DMSO. Detailed results are displayed in Figures S9–14, and Table S3, Supporting Information. The upfield shift of resonances of amine protons of the guests (g1 and g3) in DMSO- d_6 could provide more interaction information on HMeQ[7] with guests. Herein, we focus on the effect of HMeQ[7] on the solubility of drugs and select three representative drugs, namely 2-(4-thiazolyl)benzimidazole (TBZ), fuberidazole (FBZ), and carbendazim (CBZ), which display poor water solubility and contain a common benzimidazole moiety. Although it is difficult to obtain an ideal 1H NMR spectrum of neat drugs because of their poor water solubility (see Figure 3e), satisfactory 1H NMR spectra

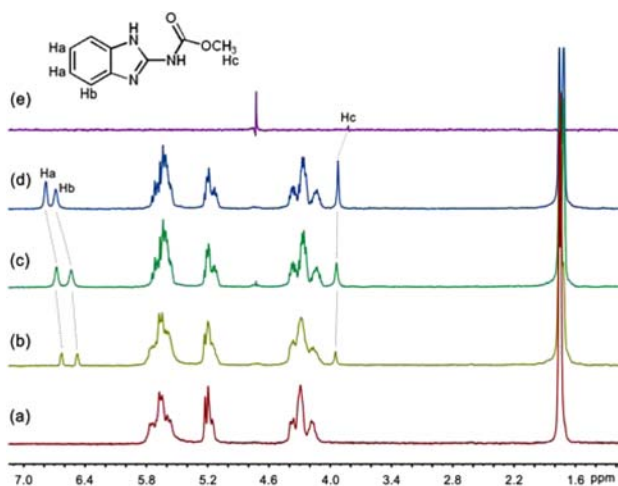


Figure 3. Titration 1H NMR spectra (400 MHz, D_2O) of host HMeQ[7] (3.97×10^{-3} mol/L) (a) in the absence and in the presence of (b) 5.56×10^{-4} mol/L, (c) 3.17×10^{-3} mol/L, and (d) 4.21×10^{-3} mol/L of CBZ in D_2O at $20^\circ C$; (e) neat CBZ (almost no signals).

were obtained to provide sufficient information in the presence of HMeQ[7]. This suggests the ability of HMeQ[7] to enhance the solubility of these drugs (refer to Figures 3b–d and S15, S16, Supporting Information). Titration 1H NMR experiments, similar to those for the guests g1–3, show some common results: (1) All three HMeQ[7]–drug interaction systems have a high binding and unbinding exchange ratio on the NMR time scale; therefore, only one set of proton resonances of the guest

was observed in the corresponding 1H NMR spectra; (2) HMeQ[7] includes the benzimidazole moiety of these representative drugs selectively; therefore, the proton signals of the benzimidazole moiety displayed a gradual downfield shift with increasing guest concentration, whereas the proton signals of the remaining guests displayed a gradual upfield shift with increasing guest concentration. This suggests that the other portion of guests was set at the HMeQ[7] molecule portal. For example, Figure 3 shows titration 1H NMR spectra obtained by using a fixed amount of HMeQ[7] and various equivalents of CBZ. A faster binding and unbinding exchange rate on the NMR time scale resulted in average CBZ proton resonances. The proton signals of the benzimidazole moiety experience a gradual downfield shift with increasing amount of CBZ, whereas the methyl proton signal experienced a gradual upfield shift with an increasing amount of CBZ.

Using a phase solubility method could provide quantitative data on how the HMeQ[7] host influences the solubility of these selected drugs. In general, the three drugs are sparingly soluble in neutral aqueous solution with solubility S_0 2.66 mg, 9.46 mg, and 0.588 mg, at $25^\circ C$. The solubility of all three drugs increased linearly as a function of HMeQ[7] and Q[7] for comparison (refer to Figure 4). The phase solubility diagrams are classified as type A_L by Higuchi and Connors, which denoted a linear increase in solubility.²⁵

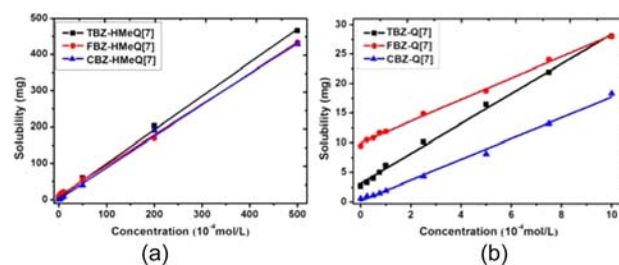


Figure 4. Phase solubility of three drugs versus concentrations of (a) HMeQ[7] and (b) Q[7] obtained in neutral water at $25^\circ C$.

Compared with the unbinding drug solubility, the concentration in the presence of HMeQ[7] at least reached 22.4 mM for CBZ, 23.5 mM for FBZ, and 23.2 mM for TBZ, which are 728-, 46-, and 175-fold increases for CBZ, FBZ, and TBZ, over those in neutral water, respectively (refer to Tables S4–S6, Supporting Information). Compared with the binding drug solubility with Q[7], a 31-, 3-, and 10-fold increase in neutral water results for HMeQ[7]–CBZ, HMeQ[7]–FBZ, and HMeQ[7]–TBZ, respectively (refer to Tables S4–S6, Supporting Information). Thus, the HMeQ[7] could display better behavior than Q[7] in enhancement of drug solubility, at least for the drugs used in this work.

On the basis of the phase solubility diagrams, the inclusion constants (K) for the six inclusion complexes were determined using eq 1, and assuming a 1:1 stoichiometry. The association constants (K) of these inclusion complexes are $(2.09 \pm 0.01) \times 10^5$ for HMeQ[7]–CBZ and $(7.58 \pm 0.14) \times 10^4$ for Q[7]–CBZ, $(1.01 \pm 0.01) \times 10^4$ for HMeQ[7]–FBZ and $(4.31 \pm 0.06) \times 10^3$ for Q[7]–FBZ, and $(9.89 \pm 0.01) \times 10^4$ for HMeQ[7]–TBZ and $(6.56 \pm 0.4) \times 10^3$ for Q[7]–TBZ.

$$K_a = \frac{\text{Slope}}{S_0(1 - \text{slope})} \quad (1)$$

In summary, we have isolated and characterized a novel hemimethyl-substituted cucurbit[7]uril (HMeQ[7]) derived from 3 α -methyl-glycoluril. Although the hemimethyl-substituted cucurbit[7]uril (HemiMeQ[7]s) could adopt 10 geometric isomers due to different orientations of the protruding methyl groups, fewer were probably formed. The HMeQ[7] molecule shows extraordinary solubilities in water and DMSO and excellent host–guest interaction properties, suggesting that it could be extensively used in drug delivery, anesthesiology, developing controllable light-harvesting systems, etc. More detailed investigations of the host–guest chemistry and coordination chemistry of HMeQ[7] are currently underway.

■ ASSOCIATED CONTENT

Supporting Information

The Supporting Information is available free of charge on the ACS Publications website at DOI: [10.1021/acs.orglett.5b02588](https://doi.org/10.1021/acs.orglett.5b02588).

General experimental procedures and analytical data for all new compounds (PDF)
X-ray data for compound 1 (CIF)

■ AUTHOR INFORMATION

Corresponding Authors

*E-mail: zqjgz@126.com.

*E-mail: gzutao@263.net.

Notes

The authors declare no competing financial interest.

■ ACKNOWLEDGMENTS

We thank the National Natural Science Foundation of China (Grant No. 21272045, 21202026), for support of this work.

■ REFERENCES

- (1) Isaacs, L. *Acc. Chem. Res.* **2014**, *47*, 2052.
- (2) Ghale, G.; Nau, W. M. *Acc. Chem. Res.* **2014**, *47*, 2150.
- (3) Kaifer, A. E. *Acc. Chem. Res.* **2014**, *47*, 2160.
- (4) Assaf, K. I.; Nau, W. M. *Chem. Soc. Rev.* **2015**, *44*, 394.
- (5) Ghosh, I.; Nau, W. M. *Adv. Drug Delivery Rev.* **2012**, *64*, 764.
- (6) Ni, X. L.; Xiao, X.; Cong, H.; Liang, L. L.; Cheng, K.; Cheng, X. J.; Ji, N. N.; Zhu, Q. J.; Xue, S. F.; Tao, Z. *Chem. Soc. Rev.* **2013**, *42*, 9480.
- (7) Lü, J.; Lin, J. X.; Cao, M. N.; Cao, R. *Coord. Chem. Rev.* **2013**, *257*, 1334.
- (8) Day, A. I.; Arnold, A. P. *Method for synthesis cucurbiturils*, WO 0068232, 2000, 8.
- (9) Kim, J.; Jung, I. S.; Kim, S. Y.; Lee, E.; Kang, J. K.; Sakamoto, S.; Yamaguchi, K.; Kim, K. *J. Am. Chem. Soc.* **2000**, *122*, 540.
- (10) Hennig, A.; Bakirci, H.; Nau, W. *Nat. Methods* **2007**, *4*, 629.
- (11) Zeng, Y.; Li, Y.; Li, M.; Yang, G.; Li, Y. *J. Am. Chem. Soc.* **2009**, *131*, 9100.
- (12) Day, A. I.; Collins, J. G. *Supramol. Chem.* **2012**, *3*, 983.
- (13) Macartney, D. H. *Future Med. Chem.* **2013**, *5*, 2075.
- (14) Jon, S. Y.; Selvapalam, N.; Oh, D. H.; Kang, J. K.; Kim, S. Y.; Jeon, Y. J.; Lee, J. W.; Kim, K. *J. Am. Chem. Soc.* **2003**, *125*, 10186.
- (15) Lee, D. W.; Park, K. M.; Banerjee, M.; Ha, S. H.; Lee, T.; Suh, K.; Paul, S.; Jung, H.; Kim, J.; Selvapalam, N.; Ryu, S. H.; Kim, K. *Nat. Chem.* **2011**, *3*, 154.
- (16) Zou, C. J.; Gu, T.; Xiao, P. F.; Ge, T. T.; Wang, M.; Wang, K. *Ind. Eng. Chem. Res.* **2014**, *53*, 7570.
- (17) Vinciguerra, B.; Cao, L.; Cannon, J. R.; Zavalij, P. Y.; Fenselau, C.; Isaacs, L. *J. Am. Chem. Soc.* **2012**, *134*, 13133.
- (18) Robinson, E. L.; Zavalij, P. Y.; Isaacs, L. *Supramol. Chem.* **2015**, *27*, 288.
- (19) Yu, Y.; Li, J.; Zhang, M. M.; Cao, L. P.; Isaacs, L. *Chem. Commun.* **2015**, *51*, 3762.
- (20) Lin, J. X.; Zhang, Y. Q.; Zhang, J.; Xue, S. F.; Zhu, Q. J.; Tao, Z. *J. Mol. Struct.* **2008**, *875*, 442.
- (21) Wang, C. Z.; Zhao, W. X.; Zhang, Y. Q.; Xue, S. F.; Tao, Z.; Zhu, Q. J. *ChemPlusChem* **2015**, *80*, 1052.
- (22) Zhang, D. Q.; Sun, T.; Zhang, Y. Q.; Xue, S. F.; Zhu, Q. J.; Zhang, J. X.; Tao, Z. *Eur. J. Inorg. Chem.* **2015**, *2015*, 318.
- (23) Li, Q.; Zhang, Y. Q.; Zhu, Q. J.; Xue, S. F.; Tao, Z.; Xiao, X. *Chem. - Asian J.* **2015**, *10*, 1159.
- (24) Ni, X. L.; Xiao, X.; Cong, H.; Zhu, Q. J.; Xue, S. F.; Tao, Z. *Acc. Chem. Res.* **2014**, *47*, 1386.
- (25) Higuchi, T.; Connor, K. A. *Adv. Anal. Chem. Instrum.* **1965**, *4*, 117.